Journal of the Korean Physical Society, Vol. 67, No. 7, October 2015, pp. 1240∼1245

Effect of Donor Doping on the Ferroelectric and the Piezoelectric Properties of Lead-free 0.97($Bi_{0.5}Na_{0.5}Ti_{1-x}Nb_x$)$O_3-0.03BaZrO_3$ Ceramics

Jamil Ur Rahman
School of Advanced Material Engineering, Changwon National University, Changwon 51140, Korea and Energy & Environmental Division, Korea Institute of Ceramic Engineering & Technology, Jinju 52861, Korea

Ali Hussain, Adnan Maqbool, Rizwan Ahmed Malik, Tae Kwon Song and Myong Ho Kim*
School of Advanced Material Engineering, Changwon National University, Changwon 51140, Korea

Soonil Lee
Energy & Environmental Division, Korea Institute of Ceramic Engineering & Technology, Jinju 52861, Korea

Won Jeong Kim
Department of Physics, Changwon National University, Changwon 51140, Korea

(Received 17 June 2015, in final form 10 July 2015)

Lead-free piezoelectric 0.97($Bi_{0.5}Na_{0.5}Ti_{1-x}Nb_x$)$O_3-0.03BaZrO_3$ (BNT-BZ3) ceramics (x = 0 ∼ 0.03) were prepared by a conventional solid-state reaction method. X-ray diffraction patterns revealed the formation of single-phase perovskite structure with $x \leq 0.015$. The depolarization temperature and the dielectric constant decreased with increasing Nb content. The remanent polarization (Pr) and the piezoelectric constant (d_{33}) increased from 28 $\mu C/cm^2$ and 98 pC/N for x = 0 to 31 $\mu C/cm^2$ and 128 pC/N for x = 0.005, respectively. In addition, the electric field induced strain was enhanced with a maximum value $S_{max} = 0.17\%$ with a normalized piezoelectric coefficient of d^*_{33} = 283 pm/V at an applied electric field of 6 kV/mm for x = 0.015.

PACS numbers: 77.65.-j, 77.90.+k
Keywords: Lead-free ceramics, BNT, Perovskite structure, Field-induced strain
DOI: 10.3938/jkps.67.1240

I. INTRODUCTION

In the past decade, lead-based piezoelectric ceramics have dominated the commercial market due to their outstanding piezoelectric, dielectric, ferroelectric and electro-mechanical properties [1–4]. However, due to the toxicity and environmental pollution causing by lead (Pb), there is an increasing demand to replace them with lead-free alternatives [5–11]. Therefore, much research attention have been given to the fabrication of new and non-polluting materials for the piezoelectric industry.

Among lead-free-bismuth based perovskite ceramics, bismuth sodium titanate, $Bi_{0.5}Na_{0.5}TiO_3$ (BNT), is considered one of the most promising candidate materials for piezoelectric applications. This material has a perovskite structure and exhibits two structural phase transitions: one from a ferroelectric rhombohedral ($R3c$) to a tetragonal ($P4bm$) phase (around 260 − 350 °C) and the other to paraelectric high temperature cubic ($Pm\bar{3}m$) phase (around 520 − 540 °C) [12–15]. However, this material has drawbacks such as its high electrical conductivity and high coercive field (E_c = 73 kV/cm), which cause problems in the poling process and thus limit its practical applications [15–17]. Such barriers were found to be overcome by forming solid solutions with other types of perovskite such as $BaTiO_3$ (BT) [15], $BaZrO_3$ (BZ) [18, 19] Ba(Zr,Ti)O_3 (BZT) [20], $SrZrO_2$ (SZ) [21], $BaNb_2O_6$ (BN) [22], $NaNbO_3$ (NN), $KNbO_3$ (KN) [23,24], $SrTiO_3$ (ST) [25], $K_{0.5}Na_{0.5}NbO_3$ (KNN) [26], *etc.* Furthermore, it has been also modified with divalent (Ca, Sr, Ba) [27] and trivalent (La, Nd, Ho, Yb) [28] ions. These modifications reveal a significant enhancement in the piezoelectric and ferroelectric behaviors of BNT ceramics.

Yeo *et al.* investigated the effects of Nb^{5+} doping on BNT ceramics and found that the donor doping of Nb^{5+} enhanced the piezoelectric and the ferroelectric properties [29]. Nb^{5+} partially substituted for Ti has also been found to be very effective in enhancing the field-induced strain response in BNT-based systems [30, 31]. In this work, we have partially substi-

*E-mail: mhkim@changwon.ac.kr; Fax: +82-55-262-6486

tuted Nb^{5+} in $Bi_{0.5}Na_{0.50}TiO_3$-0.03$BaZrO_3$ (BNT-BZ3) ceramics to develop a new lead-free piezoelectric ceramic system. Therefore, in this study, we investigated the effects of B-site donor doping (Nb^{5+}, often referred to as "soft" dopant) on $0.97(Bi_{0.5}Na_{0.5}Ti_{1-x}Nb_x)O_3-0.03BaZrO_3$ (BNT-BZ3) ceramics with x ranging from 0 to 0.03. All compositions were prepared by a conventional mixed-oxide route, and systematically studied their crystal structure, microstructure, ferroelectric, dielectric, and field-induced strain properties.

II. EXPERIMENTAL PROCEDURE

$0.97(Bi_{0.5}Na_{0.5}Ti_{1-x}Nb_x)O_3-0.03BaZrO_3$ (BNT-BZ3) ceramics with ($x = 0 \sim 0.03$) were fabricated by using a conventional solid-state reaction method. Stoichiometric ratios of Bi_2O_3 (99.90%), Na_2CO_3 (99.95%), $BaCO_3$ (99%), TiO_2 (99.90%), Nb_2O_5 (99.90%) and ZrO_2 (99%) purified form Sigma Aldrich Co., St. Louis MO were carefully weighed in accordance with the desired compositions. The mixtures were milled for 24 h with zirconia balls as a milling media in ethanol. The resulting slurry was dried at ∼90 °C overnight and then sieved and calcined at 850 °C for 2 hour at a heating/cooling rate of 5 °C/min. The calcined powders were re-milled for 24 h to reduce the particle size and dissociate agglomerates. The slurries were dried, sieved and pressed into 10-mm-diameter pellets using polyvinyl alcohol (PVA) as a binder. The pellets were sintered at 1160 °C for 2 h in air at a heating/cooling rate of 5 °C/min. To compensate the evaporation of the volatile elements (Bi and Na), green pellets were embedded in the powder of the same composition.

The phase analysis of the sintered samples was carried out using a Philips X-ray diffractometer (X'pert MPD 3040, Philips, Netherland) with Cu Ka radiation. The microstructural characterization of highly polished and thermally etched samples was performed using a JP/JSM 5200 (Japan) scanning electron microscope (SEM). The sintered samples were coated with silver paste on both faces and subsequently fired at 650 °C for 30 min to cure electrodes. For measurement of the dielectric and the piezoelectric properties, the samples were poled in a silicone oil bath with a dc field of 4 kV/mm for 30 min. All the electrical measurements were performed after the samples had been aged at least 24 h. The dielectric constant and the dielectric loss of the final ceramics were measured using an automatic acquisition system with an impedance analyzer (Agilent HP4292A, USA) at 25 – 450 °C and different frequencies. The piezoelectric constants were measured using a Berlincourt d_{33} meter (IACAS, ZJ-6B). The ferroelectric hysteresis loops were measured with a Precision Premier II equipment (Radiant Technology, Inc.). The induced strain curves were obtained using a contact-type displacement sensor (Millitron: Model 1240).

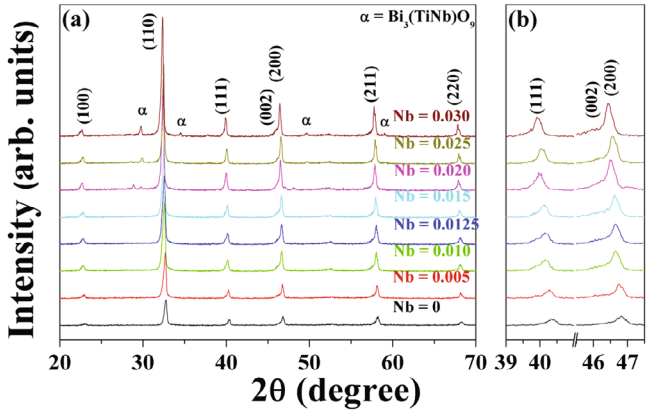

Fig. 1. (Color online) X-ray diffraction patterns of $0.97(Bi_{0.5}Na_{0.5}Ti_{1-x}Nb_x)O_3-0.03BaZrO_3$ ceramics.

III. RESULTS AND DISCUSSION

The X-ray diffraction patterns of Nb-modified BNT-BZ3 ceramics are presented in Fig. 1(a). The XRD patterns revealed the formation of a single phase perovskite structure for compositions with $x \leq 0.015$. However, with further increases in Nb content *i.e.*, $x \geq 0.020$, a couple impure phases ($\alpha = Bi_3(TiNb)O_9$) of low-intensities were emerged, which confirmed the solubility limit of Nb^{5+} in the BNT-BZ3 ceramics. Figure 1(b) shows magnified XRD patterns in the 2θ range 39° – 41° and 45° – 48°. For those patterns around 46° a slight peak splitting (002)/(200) was observed. In addition, with the incorporation of Nb in BNT-BZ3, a shift of the peaks towards lower angles was observed. This suggests that Nb substitution into BNT-BZ3 led to expansion of the unit cell [25, 32] due to the substitution Nb^{5+} with a lager ionic radius of 0.69 Å for Ti^{4+} with a smaller ionic 0.605 Å at B-site of BNT-BZ3 lattice.

Figure 2 presents the SEM micrographs of Nb-modified BNT-BZ3 ceramics sintered at 1160 °C for 2 h. All samples show very dense, uniformly-distributed, tightly-bound and homogeneous microstructures. Clearly, an increase in Nb^{5+} content had no remarkable effect on the grain's morphology. However, it decreased the average grain size of the BNT-BZ3 ceramics significantly. In view of defect chemistry, the following equation should considered:

$$2Nb_2O_5 + 2Bi_2O_3 \rightarrow 2Bi^X_{Bi} + 4Nb^{\bullet}_{Ti} + 2V'''_{Bi} + V^{\bullet\bullet}_O + 11O^X_O + 2O_2(g). \quad (1)$$

The slight decrease in the grain size may be due to an excess of A-site cation vacancies and a suppression of oxygen vacancies with increasing B-site donor doping. A similar behavior was also reported in Nb-doped BNT ceramics [29].

Figure 3 shows the temperature dependences of the dielectric constant (ε_r) and the dielectric loss ($\tan\delta$) of poled Nb-modified BNT-BZ3 ceramics at different fre-

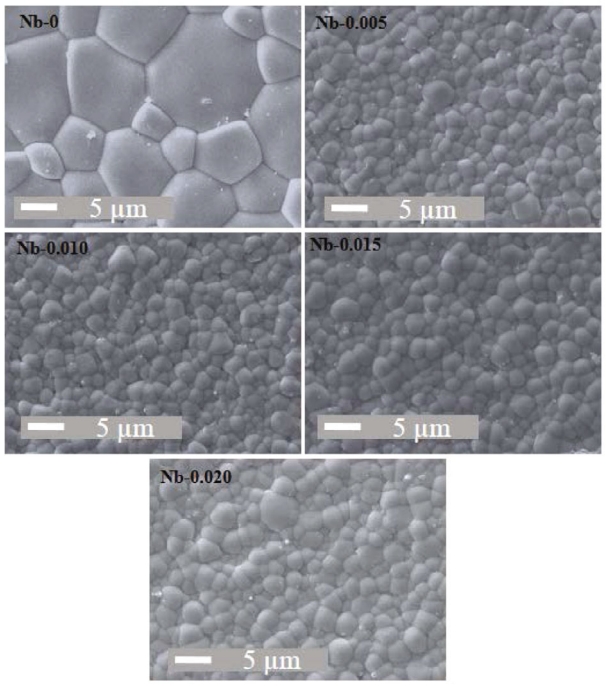

Fig. 2. SEM micrographs of 0.97 $(Bi_{0.5}Na_{0.5}Ti_{1-x}Nb_x)O_3-0.03BaZrO_3$ ceramics with different Nb^{5+} contents.

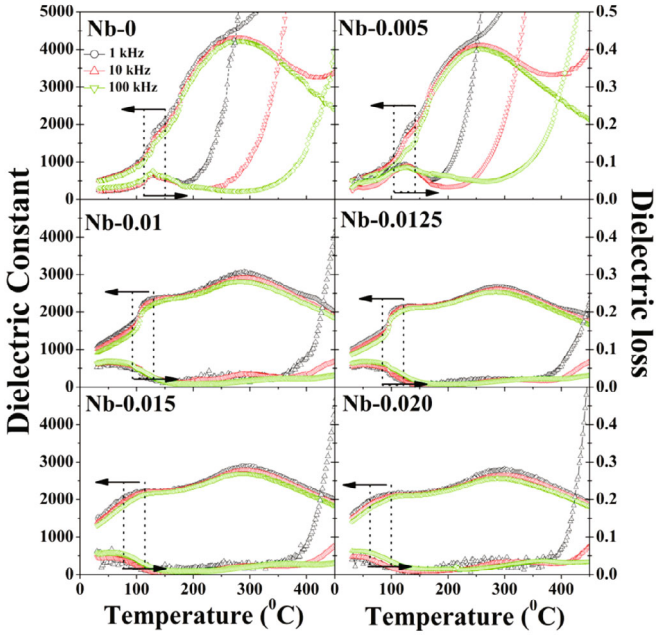

Fig. 3. (Color online) Temperature dependences of the dielectric constant and loss of poled 0.97$(Bi_{0.5}Na_{0.5}Ti_{1-x}Nb_x)O_3-0.03BaZrO_3$ ceramics with $x = 0$, 0.005, 0.010, 0.0125, 0.015 and 0.020 at various frequencies.

quencies (1, 10, and 100 kHz). As can be seen in Fig. 3, two dielectric anomalies are present in the ε_r − T curve of unmodified BNT-BZ3 ceramics. The first is the hump at about 130 °C known as the depolarization temperature (T_d), at which the ferroelectricity is significantly decreased. The other at which the dielectric constant reaches its maximum value is at about 275 °C that is known as the maximum dielectric constant temperature (T_m). This dielectric behavior observed in Nb modified BNT-BZ3 ceramics is consistent with previous reports on BNT-based ceramics [33–35]. The dielectric anomalies were clearly affected by Nb-modification. The first inflection point T_d decreases from 130 °C to 55 °C as the Nb content is increased from 0 to 0.020, respectively. On the other hand, the second inflection point, T_m, exhibits diffused phase transition and is shifted toward higher temperature, which is similar to that of Nb-doped BNKT ceramics [31]. The Nb-modified BNT-BZ3 ceramics is also noted to show relaxor characteristics; both transition temperatures, T_d and T_m, are strongly depend on the frequency. The higher the frequency is, the lower the value of the dielectric constant value is.

In addition, the dielectric loss curves show that at a temperature around 200 °C at 1 kHz for $x = 0$, a sharp increase is observed in the loss curve which shifts toward higher temperature at the higher frequencies. This dispersion of the dielectric peak also shifts toward higher temperature with increasing Nb content, except $x = 0.005$. The dielectric loss mainly results from the domain walls in BNT-based ferroelectric ceramics, and with increasing temperature macro-domains change to micro-domains and the domain walls sharply increase, which leads to a dramatic increase of dielectric loss [36]. However, in the Nb-modified BNT-BZ3 with $x = 0$ and 0.005, the significant increases in the dielectric constant and loss with decreasing frequency is believed to indicate a space charge effect and conduction by an ionic species, such as oxygen vacancies, and by ionic migration. With further increases in the Nb content, the number of oxygen vacancies can be suppressed further by partial charge-compensation on Bi vacancies with increasing Nb substitution into Ti sites, as shown in Eq. (1), which presumably contributes to the lower the dielectric loss in the Nb-modified BNT-BZ3 with $x > 0.005$.

To investigate the ferroelectric response of Nb-modified BNT-BZ3 ceramics, polarization hysteresis (P-E) loops were measured at room temperature. Figure 4(a) shows that the (P-E) curves were significantly affected with Nb content. The ceramic with $x = 0$ exhibits a typical ferroelectric behavior with a remanent polarization of $P_r = 28$ $\mu C/cm^2$, a coercive field ($E_c = 3.7$ kV/mm) and a maximum polarization of $P_m = 32$ $\mu C/cm^2$. However, with the addition of a small amount of Nb ($x = 0.005$), Pr increased to 31 $\mu C/cm^2$ and then decreases with further increase in the Nb content. The coercive field continuously decreased with increasing Nb content. The characteristic values of P_r, P_m, and E_c are shown in Fig. 4(b). The observed ferroelectric properties indicate that the introduction of a small amount of Nb^{5+} improves the ferroelectricity of the BNT-BZ3 ceramic. The decrease in the E_c can also be correlated with donor doping. In general, oxygen vacancies and

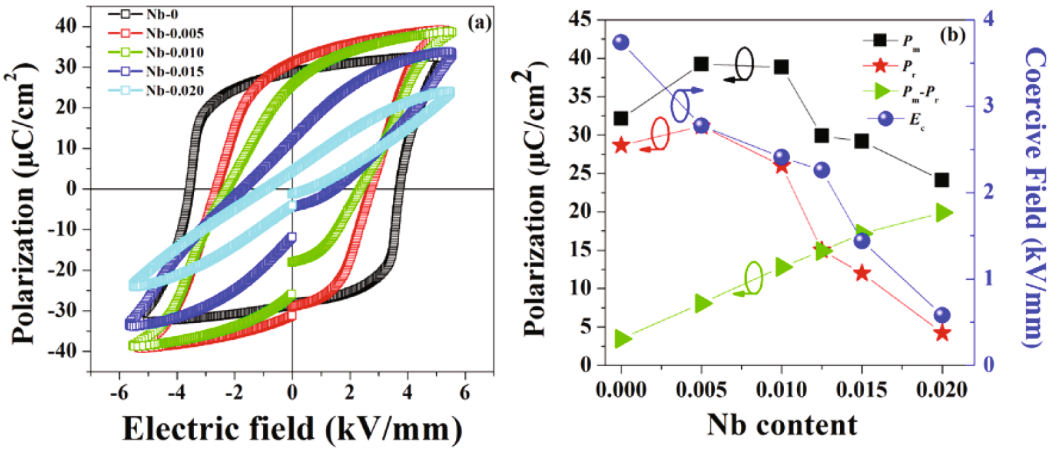

Fig. 4. (Color online) Room-temperature ferroelectric properties: (a) *P-E* loops of $0.97(Bi_{0.5}Na_{0.5}Ti_{1-x}Nb_x)O_3$-$0.03BaZrO_3$ ceramics with $x = 0$, 0.005, 0.010, 0.015 and 0.020; (b) polarization and coercive field of $0.97(Bi_{0.5}Na_{0.5}Ti_{1-x}Nb_x)O_3$-$0.03BaZrO_3$ ceramics as a function of the Nb content.

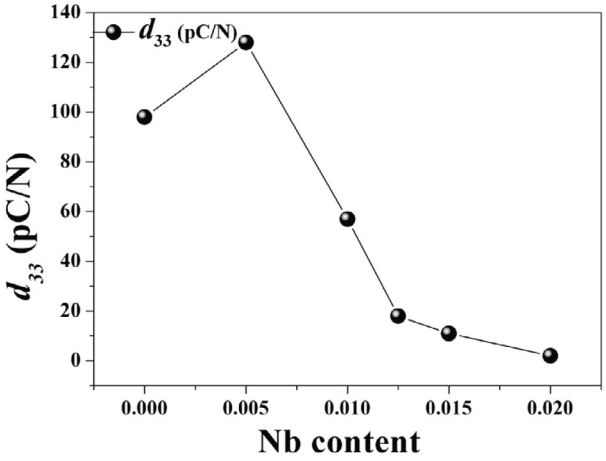

Fig. 5. Piezoelectric constant (d_{33}) of $0.97(Bi_{0.5}Na_{0.5}Ti_{1-x}Nb_x)O_3$-$0.03BaZrO_3$ ceramics with different Nb contents.

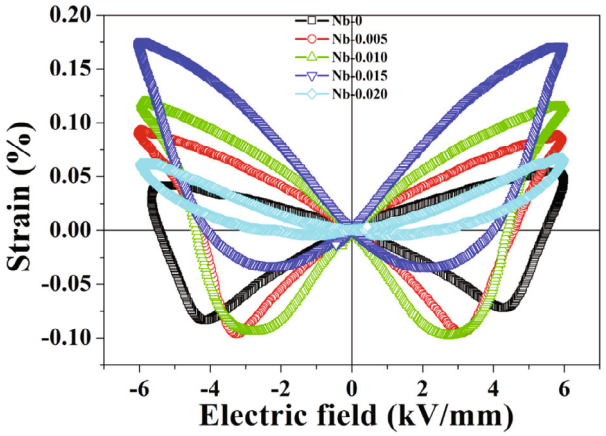

Fig. 6. (Color online) Room-temperature bipolar field-induced strain response of $0.97(Bi_{0.5}Na_{0.5}Ti_{1-x}Nb_x)O_3$-$0.03BaZrO_3$ ceramics with $x = 0$, 0.005, 0.015 and 0.020 for electric field of 6 kV/mm.

associated defect complexes, which can pin the domain walls and the grain boundaries, lead to high value of E_c and large grains, respectively. However, with increasing Nb^{5+} doping, the oxygen vacancies is suppressed by partial charge-compensation of Bi vacancies with Nb substitution into Ti sites, as shown in Eq. (1), which yields low value of E_c and small grain sizes. Furthermore, the large decreases in both P_r and E_c may suggest the typical behavior observed in relaxor ferroelectrics (RFE). At a higher concentration of Nb^{5+}, this relaxor-type behavior becomes dominant due to the significant reduction in the polarization states (P_m, P_r and E_c).

Figure 5 shows the dependence of the piezoelectric constant (d_{33}) of the Nb-modified BNT-BZ3 ceramics at room temperature. The d_{33} parameter increases from 98 pC/N for $x = 0$ to 128 pC/N $x = 0.005$. However, with further increases in the Nb^{5+} content, the d_{33} decreases. This trend of d_{33} is in good agreement with the ferroelectric response (see Fig. 4). The significant improvement observed in d_{33} at $x = 0.005$ is attributed to the large remanent polarization (P_r) and the lower coercive field (E_c). This is because a lower value of E_c enables the ceramics to be more easily poled while a large P_r favors piezoelectricity.

Bipolar field-induced strain (*S-E*) curves for the Nb-modified BNT-BZ3 ceramics measured at room temperature under applied electric field of 6 kV/mm are provided in Fig. 6 for compositions $x = 0$, 0.005, 0.015, and 0.020. The pure BNT-BZ3 ceramics exhibit a butterfly-shaped curve with maximum (S_{max}) and negative strains (S_n) of 0.05% and 0.07%, respectively, showing a typical ferroelectric behavior. However, with the addition of a small amount of Nb^{5+}, the ferroelectric order is disturbed, and the curves changed to relaxor-type curves,

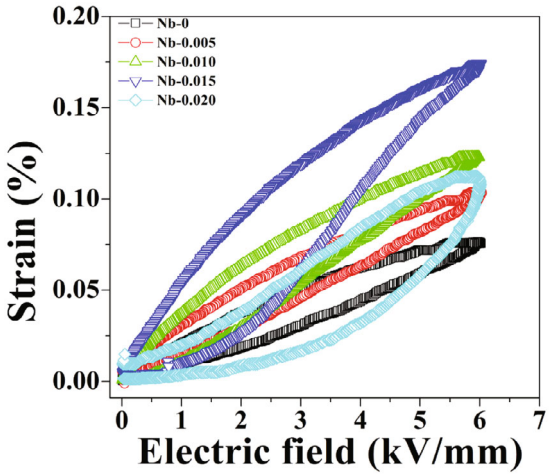

Fig. 7. (Color online) Unipolar field-induced strain curves of $0.97(Bi_{0.5}Na_{0.5}Ti_{1-x}Nb_x)O_3$-$0.03BaZrO_3$ ceramics with different Nb^{5+} content.

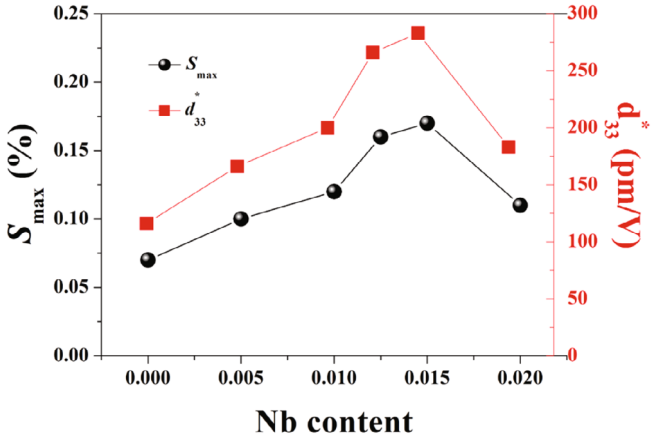

Fig. 8. (Color online) Characteristic values of the maximum strain and the normalized strain of 0.97 $(Bi_{0.5}Na_{0.5}Ti_{1-x}Nb_x)O_3$-$0.03BaZrO_3$ ceramics as a function of the Nb content.

resulting in an increase in the maximum strain up to $x = 0.015$ and then a decrease. Consequently, a maximum bipolar strain ($S_{max} = 0.17\%$) and a small negative strain ($S_n = 0.03\%$) were exhibited because of Nb doping in the BNT-BZ3 ceramics.

Figure 7 shows the unipolar field-induced strain curves for BNT-BZ3 ceramics with different Nb^{5+} concentrations measured at room temperature under applied electric field of 6 kV/mm. Similar to the bipolar strain, the unipolar strain also increases with increasing Nb^{5+} concentration up to $x = 0.015$ and then decreases. The maximum unipolar strain level increases from 0.07% to 0.17% for $x = 0$ to $x = 0.015$. Their corresponding normalized strain ($d^*_{33} = S_{max}/E_{max}$) values increase from 116 pm/V to 283 pm/V. However, with further increase in Nb^{5+} content, the field-induced strain level drops. The maximum field-induced strain along with the normalized strain of Nb-modified BNT-BZ3 ceramics are presented in Fig. 8. The field-induced strain level and its corresponding normalized strain in this study are higher than the values previously reported for BNT-based binary systems [15,24]. Clearly, that Nb^{5+} is an effective material to improve the ferroelectric and the piezoelectric properties of BNT-BZ3 ceramics.

IV. CONCLUSION

The effect of Nb^{5+} on the crystal structural, microstructural, dielectric, ferroelectric and field-induced strain behaviors of $0.97(Bi_{0.5}Na_{0.5}Ti_{1-x}Nb_x)O_3$-$0.03BaZrO_3$ (BNT-BZ3) ceramics was investigated. XRD patterns revealed the formation of a single-phase perovskite structure for compositions with $x \leq 0.015$. The depolarization temperature T_d gradually decreased with increasing Nb^{5+} content. The ferroelectric and the piezoelectric properties were enhanced with a high P_r = 31 $\mu C/cm^2$, a low E_c of 2.7 kV/mm and a high d_{33} = 128 pC/N, all of which were observed at $x = 0.005$. A large field-induced strain of 0.17% with a normalized strain d^*_{33} of 283 pm/V was observed for $x = 0.015$.

ACKNOWLEDGMENTS

This research work was financially supported by Changwon National University 2014 ∼ 2015 and National Research Foundation of Korea (NRF) grant funded by the Korean government, Ministry of Education (MOE, 2013R1A1A2058345).

REFERENCES

[1] K. Uchino, Piezoelectric actuators and ultrasonic motors, (Springer US, 1996).
[2] J. F. Tressler, S. Alkoy and R. E. Newnham, J. Electroceram. **2**, 257 (1998).
[3] B. Jaffe, W. R. Cook and H. Jaffe, *Piezoelectric ceramics* (Academic Press London, 1971).
[4] N. Ichinose, N. Miyamoto and S. Takahashi, J. Eur. Ceram. Soc. **24**, 1681 (2004).
[5] E. Directive, Official Journal of the European Union **13**, L37 (2003).
[6] Y. Saito, H. Takao, T. Tani, T. Nonoyama, K. Takatori, T. Homma, T. Nagaya and M. Nakamura, Nature **432**, 84 (2004).
[7] E. Cross, Nature **432**, 24 (2004).
[8] J. Wu, Y. Wang, D. Xiao, J. Zhu and Z. Pu, Appl. Phys. Lett. **91**, 132914 (2007).
[9] W. Liu and X. Ren, Phys. Rev. Lett. **103**, 257602 (2009).
[10] S. Zhang, R. Xia and T. R. Shrout, J. Electroceram. **19**, 251 (2007).

[11] J. Rodel, W. Jo, K. T. Seifert, E. M. Anton, T. Granzow and D. Damjanovic, J. Am. Ceram. Soc. **92**, 1153 (2009).
[12] G. Jones and P. Thomas, Acta Crystallogr., Sect. B: Struct. Sci **56**, 426 (2000).
[13] G. Jones and P. Thomas, Acta Crystallogr., Sect. B: Struct. Sci **58**, 168 (2002).
[14] J. Suchanicz, Ferroelectrics **209**, 561 (1998).
[15] T. Takenaka, K. I. Maruyama and K. Sakata, Jpn. J. App. Phys. **30**, 2236 (1991).
[16] G. A. Smolenskii, V. A. Isupov, A. I. Agranovskaya and N. N. Krainik, Sov. Phys. Solid State **2**, 2651 (1961).
[17] C. Peng, J. F. Li and W. Gong, Mater. Lett. **59**, 1576 (2005).
[18] J. U. Rahman, A. Hussain, A. Maqbool, T. K. Song, W. J. Kim, S. S. Kim and M. H. Kim, Curr. Appl Phys. **14**, 331 (2014).
[19] J. U. Rahman, A. Hussain, A. Maqbool, R. A. Malik, M. S. Kim and M. H. Kim, J. Korean Phys. Soc. **66**, 1072 (2015).
[20] Z. Yu, C. Ang, R. Guo and A. S. Bhalla, J. App. Phys. **92**, 1489 (2002).
[21] A. Maqbool, A. Hussain, J. U. Rahman, J. K. Park, T. G. Park, J. S. Song and M. H. Kim, Trans. Nonferrous Met. Soc. China **24**, s146 (2014).
[22] C. Zhou and X. Liu, J. Mater. Sci. - Mater. Electron **19**, 29 (2007).
[23] T. Takenaka, T. Okuda and K. Takegahara, Ferroelectrics **196**, 175 (1997).
[24] Y. Hiruma, H. Nagata and T. Takenaka, J. App. Phys. **104**, 124106 (2008).
[25] Y. Hiruma, Y. Imai, Y. Watanabe, H. Nagata and T. Takenaka, Appl. Phys. Lett. **92**, 262904 (2008).
[26] A. B. Kounga, S.-T. Zhang, W. Jo, T. Granzow and J. Rodel, Appl. Phys. Lett. **92**, 222902 (2008).
[27] Y. Watanabe, Y. Hiruma, H. Nagata and T. Takenaka, Ceram. Int. **34**, 761 (2008).
[28] Y. Hiruma, Y. Watanabe, H. Nagata and T. Takenaka, Key Eng. Mater. **350**, 93 (2007).
[29] H. G. Yeo, Y. S. Sung, T. K. Song, J. H. Cho, T. G. Park, M. H. Kim and Y. S. Sung, J. Korean Phys. Soc. **54**, 896 (2009).
[30] A. Hussain, A. Zaman, Y. Iqbal and M. H. Kim, J. Alloys Compd. **574**, 320 (2013).
[31] K. N. Pham, A. Hussain, C. W. Ahn, W. Kim, S. J. Jeong and J. S. Lee, Mater. Lett. **64**, 2219 (2010).
[32] Y. S. Sung, J. M. Kim, J. H. Cho, T. K. Song, M. H. Kim and T. G. Park, Appl. Phys. Lett. **96**, 202901 (2010).
[33] C. Xu, D. Lin and K. W. Kwok, Solid State Sci. **10**, 934 (2008).
[34] W. Krauss, D. Schütz, F. A. Mautner, A. Feteira and K. Reichmann, J. Eur. Ceram. Soc. **30**, 1827 (2010).
[35] A. Maqbool, A. Hussain, J. U. Rahman, T. K. Song, W. J. Kim, J. Lee and M. H. Kim, Ceram. Int. **40**, 11905 (2014).
[36] C. R. Zhou and X. Y. Liu, Bull. Mater. Sci. **30**, 575 (2007).